Grating detuning effect on holographic memory in photopolymers

Mei-Li Hsieh
Ken Y. Hsu, MEMBER SPIE
National Chiao Tung University
Institute of Electro-Optical Engineering
Hsin-Chu, Taiwan
E-mail: ken@cc.nctu.edu.tw

Abstract. We present a study of the grating detuning effect on the transmission and reflection holographic memories recorded in a photopolymer material. By using the Bragg matching condition, we analyze the angular shift and the degradation of the diffraction efficiency of the reconstructed images. Based on these results, a method for precompensating the detuning effect has been proposed. [DOI: 10.1117/1.1402125]

Subject terms: Bragg detuning; holographic memory; volume holograms.

Paper PT-010 received Dec. 20, 2000; revised manuscript received Feb. 8, 2001; accepted for publication Feb. 8, 2001.

1 Introduction

Holographic data storage has been considered as one of the next-generation information storage technologies because of its potential in high storage capacity ($\sim 10^{12}$ bits/cm^3) and fast readout speed ($\sim 10^{11}$ bits/sec).[1–3] Suitable recording material is a key to the success of holographic memories. So far, the most popular materials for this application are photorefractive crystals and photopolymers. Photorefractive crystals have been the traditional experimental choice because of their excellent optical quality. However, it suffers from small dynamic range and low photosensitivity. Photopolymer materials are especially interested because these materials have large refractive index contrast ($\Delta n \sim 0.01$) and high photosensitivity ($10 \sim 10^4$ J/m^2), and they can be easily synthesized to have different compositions.[4,5] However, the major disadvantage for using photopolymer materials is the grating detuning effect. This effect comes from the dimensional changes (shrinkage or expansion) induced by the chemical reactions during the holographic recording procedure, such that the recorded refractive index grating has different grating spacing from that of the light interference fringes. As a result, the Bragg condition for volume holograms is mismatched and the recorded information cannot be readout completely.[6,7] Therefore, it is important to know how the grating detuning effect influences the reconstructed image and how to alleviate this problem.[8–10]

We present a study of the grating detuning effect on holographic data storage using photopolymer recording material. By using the Bragg matching condition, we analyze the angular shift and the degradation of diffraction efficiency of the reconstructed beam. The distortion of the readout page is described, and a method for precompensation by deviating the incident angles of the reading beam from the original writing beam is proposed.

This paper is a revision of a paper presented at the SPIE conference on Optical Storage and Optical Information Processing, July 2000, Taipei, Taiwan. The paper presented there appears (unrefereed) in SPIE Proceedings Vol. 4081.

2 Theoretical Analysis

2.1 *Transmission Holograms*

2.1.1 *Angular shift of the reconstructed beam*

We first derive equations for the shift of Bragg angle due to shrinkage of the recording material for the transmission hologram. The schematic diagram of the geometry for recording a transmission hologram is shown in Fig. 1(a). In the figure, the surface of the sample is on the x-y plane and the surface normal is along the z axis. Geometrical dimensions d and l are the thickness and the transverse length of the photopolymer sample before optical exposure, respectively, and n is the refractive index. Angles θ_{1a} and θ_{2a} represent the incident angles of the reference and the object beam with respect to the z axis, respectively. All the angles are measured outside the medium. During optical recording, the interference pattern is recorded in the medium. The grating vector can be written as[11]:

$$\vec{K} = \vec{k}_2 - \vec{k}_1 = \frac{2\pi}{\Lambda}(-\cos\theta_0 \hat{x} - \sin\theta_0 \hat{z}), \tag{1}$$

where $\hat{x}$ and $\hat{z}$ are unit vectors along the x and z axis, $\theta_0 = (\theta_1 - \theta_2)/2$, and Λ is the grating spacing, given by

$$\Lambda = \frac{\lambda}{2n \sin\left(\frac{\theta_1 + \theta_2}{2}\right)}, \tag{2}$$

where λ is the optical wavelength in free space, θ_1 and θ_2 are the incident angles of the reference and object beams inside the medium, respectively. According to Snell's law, θ_1 and θ_2 can be written as $\theta_1 = \cos^{-1}[\cos(\theta_{1a})/n]$ and $\theta_2 = \cos^{-1}[\cos(\theta_{2a})/n]$.

Assume that because of the shrinkage effect, after optical exposure, the thickness and the transverse dimensions of the recording medium are changed to $(1+\alpha_d)\cdot d$ and $(1+\alpha_l)\cdot l$, where α_d and α_l are the fraction of the material

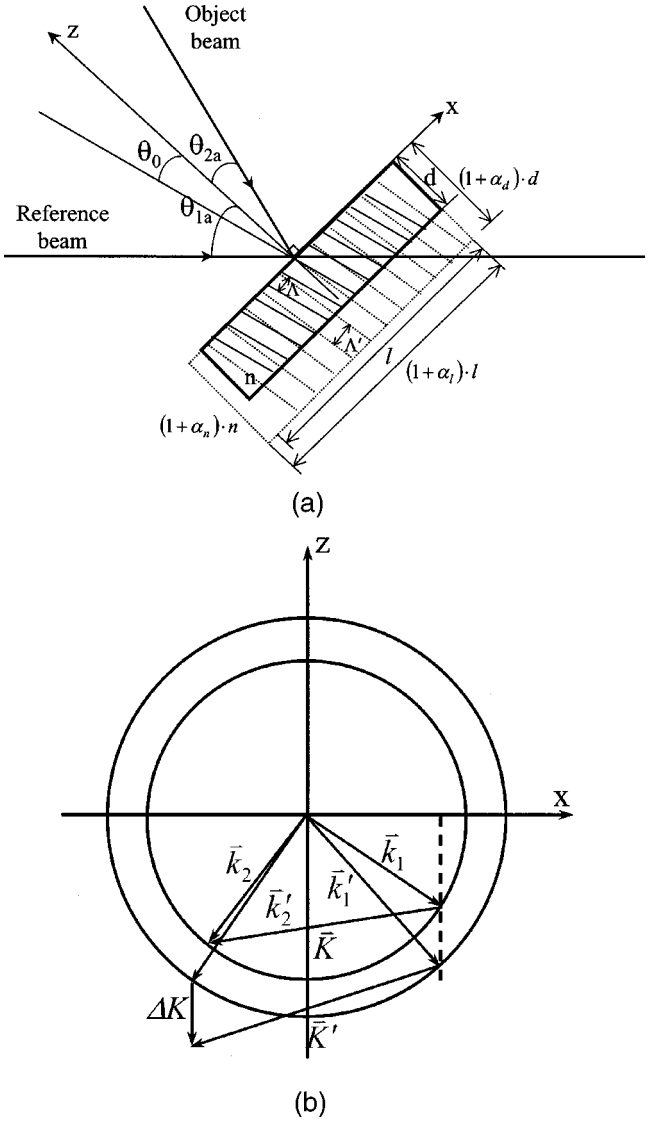

Fig. 1 (a) Schematic diagram for recording transmission hologram and (b) *K* diagram for the transmission hologram.

shrinkage along the corresponding directions. Furthermore, assume that the refractive index of the material has changed to $(1+\alpha_n)\cdot n$, where α_n is the fractional change in the refractive index. Then, the recorded grating vector is changed to

$$\vec{K}' = \frac{2\pi}{\Lambda}\left(-\frac{1}{1+\alpha_l}\cos\theta_0\hat{x} - \frac{1}{1+\alpha_d}\sin\theta_0\hat{z}\right). \tag{3}$$

Now if the holographic grating is reconstructed by the original reference beam, the Bragg matching condition will no longer be satisfied. We assume that the grating is infinite in the *x* direction so that the Bragg mismatch is along the *z* axis, as required by the boundary condition. We describe the conservation of the momentum by the *k* diagram, which is shown in Fig. 1(b). The amount of the phase mismatch ΔK can be derived as

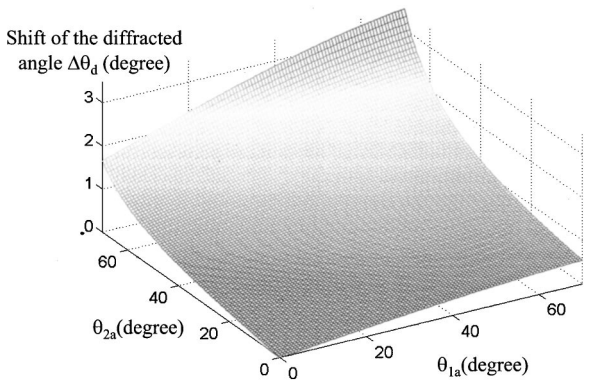

Fig. 2 Simulation results of the shift of the diffracted angle $\Delta\theta_d$ as a function of the incident angles θ_{1a} and θ_{2a}. θ_{1a} is the incident angle of the reference beam, and θ_{2a} is the incident angle of the object beam.

$$\begin{aligned}\Delta K &= k_{1z}' + K_z' - k_{dz} \\ &= \frac{2\pi}{\lambda}\Bigg(-\{[(1+\alpha_n)n]^2 - \sin^2\theta_{1a}\}^{1/2} - \frac{1}{1+\alpha_d} \\ &\quad \times[(n^2-\sin^2\theta_{2a})^{1/2} - (n^2-\sin^2\theta_{1a})^{1/2}] \\ &\quad + \Bigg\{[(1+\alpha_n)n]^2 \\ &\quad - \left[\sin\theta_{1a} - \frac{1}{1+\alpha_l}(\sin\theta_{1a}+\sin\theta_{2a})\right]^2\Bigg\}^{1/2}\Bigg),\end{aligned} \tag{4}$$

where k_{1z}' is the wave vector of the reading beam along the *z* axis and k_{dz} is the wave vector of the reconstructed beam along the *z* axis. The value of the diffracted wave vector is equal to $2\pi n(1+\alpha_n)/\lambda$. In Fig. 1(b), $k_{dx} = k_{1x}' + K_x'$; consequently, we can obtain the wave vector of the diffracted beam along the *z* axis, i.e., $k_{dz} = -\{[2\pi n(1+\alpha_n)/\lambda]^2 - (k_{dx})^2\}^{1/2}$. Thus, the diffracted angle of the reconstructed beam is deviated from the original direction. It can be derived as

$$\begin{aligned}\Delta\theta_d &= \theta_{2a}' - \theta_{2a} \\ &= \sin^{-1}\left[\frac{1}{1+\alpha_l}(\sin\theta_{1a}+\sin\theta_{2a}) - \sin\theta_{1a}\right] - \theta_{2a},\end{aligned} \tag{5}$$

where θ_{2a}' is the diffracted direction. According Eq. (5), the shift of the diffracted angle depends on the recording angles θ_{1a}, θ_{2a}, and α_l, the dimensional shrinkage along the *x* axis. If $\alpha_l = 0$, then $\Delta\theta_d = 0$, i.e., the angular shift is zero, and the diffracted beam is along the original direction of the object beam. In other words, the diffracted angle will remain unchanged if there is no shrinkage along the transverse dimension of the recording material.

We have performed a numerical calculation with $d = 100\,\mu$m, $\lambda = 514$ nm, $n = 1.5285$, $\alpha_l = -1\%$, $\alpha_d = -1\%$, and $\alpha_n = 1\%$. In this case the diffracted angles are affected. The simulation results (as shown in Fig. 2) indicate that the angular shift of the diffracted beam increases with increasing incident angles θ_{1a} and θ_{2a}. The

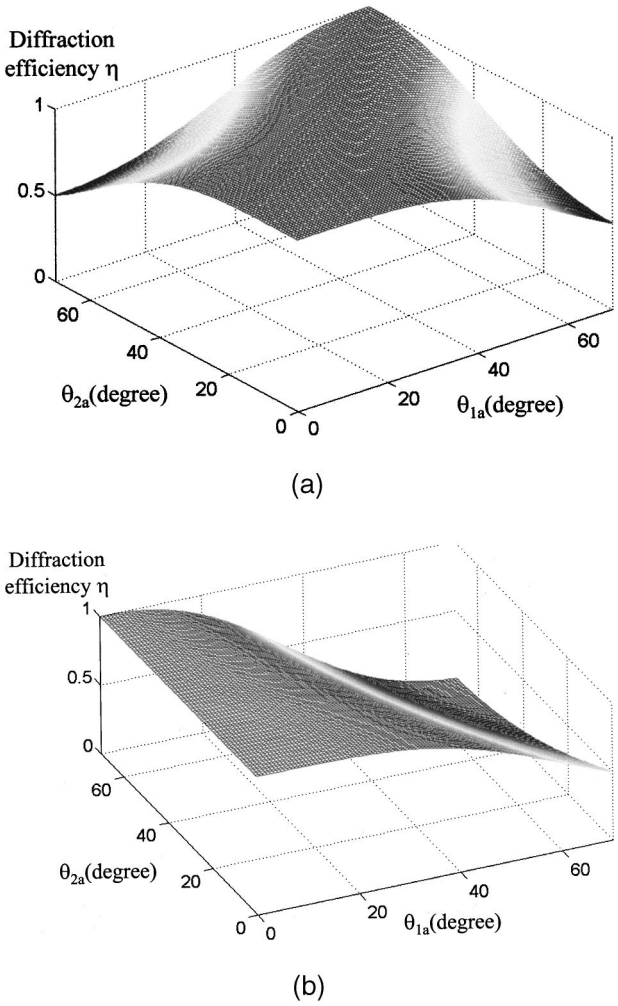

Fig. 3 (a) Simulation results of the diffraction efficiency η as a function of the incident angles θ_{1a} and θ_{2a}. θ_{1a} is the incident angle of the reference beam, and θ_{2a} is the incident angle of the object beam. (b) Simulation results of the diffraction efficiency η as a function of the incident angles θ_{1a} and θ_{2a}.

angular shifts are less than 0.98 deg when the recording angles are less than 40 deg, and the shift can be larger than 3 deg when both θ_{1a} and θ_{2a} are larger than 60 deg.

2.1.2 *Degradation of the diffraction efficiency*

The normalized diffraction efficiency of a mismatched volume holographic grating can be written as[11]

$$\eta = \mathrm{sinc}^2\left(\frac{\Delta K \cdot d}{2\pi}\right). \tag{6}$$

Equation (6) shows that in all cases of shrinkage, the diffraction efficiency will be degraded. Combining Eqs. (4) and (6) we see that the diffraction efficiency depends on the recording angles θ_{1a} and θ_{2a}. We have performed a numerical calculation. The simulation result is shown in Fig. 3(a). The parameters used for this simulation are $d = 100\,\mu$m, $\lambda = 514$ nm, $n = 1.5285$, $\alpha_l = 0$, $\alpha_d = -1\%$, and $\alpha_n = 1\%$. The simulation results show that when the incident angles of the two recording beams are symmetric, then the diffraction efficiency will remain unaffected.

Figure 3(b) considers a similar example except with $\alpha_l = -1\%$. Now the diffraction efficiency is degraded even when the incident angles of the recording beams are symmetric with respect to the surface normal. It also shows that the diffraction efficiency decreases significantly from 1 to 0.012 when both the incident angles of the reference beam (θ_{1a}) and the object beam (θ_{2a}) are increased from 0 to 70 deg. When the object beam is normally incident onto the recording material ($\theta_{2a} = 0$ deg) and the incident angle of the reference beam is less than 40 deg, the diffraction efficiency is above 0.897. Thus, in this case, the reference beam with smaller incident angles can provide higher diffraction efficiency.

Let us consider a practical example. We consider the recording and reading of a Fourier hologram. Assume that the center of the object beam is normally incident onto the recording material, and the size of the input spatial light modulator (SLM) is 13.2 mm. The pixel size of the SLM is 33 μm and there are 400 pixels in each dimension. The focal length of the lens is 40 cm. Thus, the range of the incident angles is from -0.87 to 0.87 deg. The reconstructed beam is inverse transformed and imaged onto a CCD by a lens of 20-cm focal length. The pixel size of the CCD detector is 15 μm. We used DuPont HRF-800$\times$071 photopolymer as the recording material. The thickness of this material is $d = 20\,\mu$m. The refractive index and the fractional change in refractive index are measured by an Abbe refractometer to be $n = 1.5285$ and $\alpha_n = 0.27\%$. By comparing the phase change between two arms in a Mach-Zehnder interferometer after and before optical exposure, the fractional change of the thickness is obtained as $\alpha_d = -1.5\%$. The details of the measurements are described in Sec. 3. By using Eqs. (5) and (6), the position shift and the diffraction efficiency of the reconstructed image as a function of the pixel positions are shown in Figs. 4(a) and 4(b), respectively. Figure 4(a) shows that the shift of output image decreases with smaller recording angles. Figure 4(b) shows that the distribution of the diffraction efficiency across the output image is more uniform with large recording angles. In addition, the diffraction efficiency is higher by using reference beams with larger recording angles. Note that the latter characteristic has a tendency opposite to that in Fig. 3(b) because the parameters of the photopolymers for these two cases are different. Hence, the parameters of the photopolymer are very important in considering the detuning effect of the holographic storage. Furthermore, by considering the detuning effects shown in Figs. 4(a) and 4(b), a compromise between the pixel shift and the diffraction efficiency can be achieved by appropriately choosing the recording angles.

2.1.3 *Precompensation by angular shift of the reading beam*

From the discussion in the previous paragraph, we know that because of the shrinkage effect during the recording procedure, a phase mismatch will be induced if the reading beam is incident at the original incident angle of the reference beam. To reconstruct the volume grating at the Bragg matching condition, the reading beam should be deviated

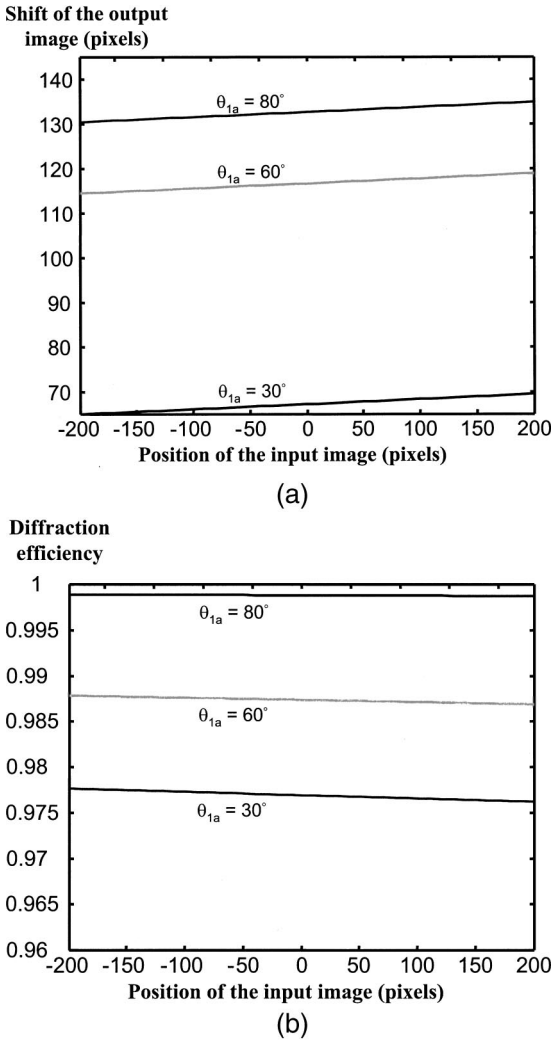

Fig. 4 (a) The position shift of the reconstructed image as a function of the image pixels with different incident angles $\theta_{1a}=80$, 60, and 30 deg. (b) The diffraction efficiency of the reconstructed image as a function of the image pixels with different incident angles $\theta_{1a}=80$, 60, and 30 deg.

from the original incident angles. This is called the precompensation process. By using the condition of conservation of the grating momentum, the required angular shift of the reading beam from the reference beam can be given as

$$\Delta\theta_r=\theta'_{1a}-\theta_{1a}$$
$$=\sin^{-1}\left\{(1+\alpha_n)n\cdot\sin\left[\sin^{-1}\left(\frac{\lambda}{2(1+\alpha_n)n\Lambda'}\right)+\tan^{-1}\left(\frac{1+\alpha_l}{1+\alpha_d}\tan\theta_0\right)\right]\right\}-\theta_{1a}, \quad (7)$$

where Λ' is the grating spacing with shrinkage and it can be described by

$$\Lambda'=\frac{\Lambda}{\left[\left(\frac{1}{1+\alpha_d}\sin\theta_0\right)^2+\left(\frac{1}{1+\alpha_l}\cos\theta_0\right)^2\right]^{1/2}}. \quad (8)$$

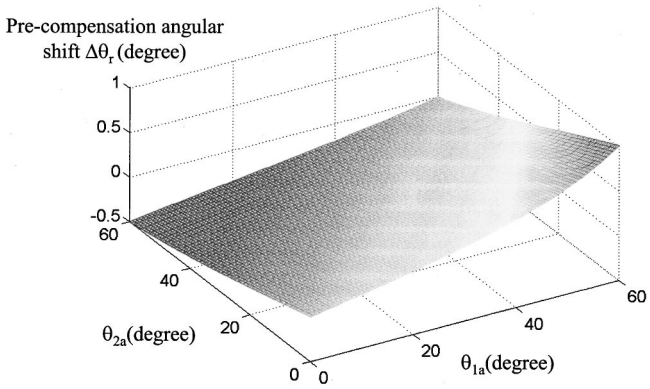

Fig. 5 Simulation results of the precompensation angular shift $\Delta\theta_r$ as a function of the incident angles θ_{1a} and θ_{2a}.

Under this situation, the diffracted angle is changed and the shift of the diffracted angle can be derived as

$$\Delta\theta_d=\theta_d-\theta_{2a}$$
$$=\sin^{-1}\left\{(1+\alpha_n)n\cdot\sin\left[\sin^{-1}\left(\frac{\lambda}{2(I+\alpha_n)n\Lambda'}\right)-\tan^{-1}\left(\frac{1+\alpha_l}{1+\alpha_d}\tan\theta_0\right)\right]\right\}-\theta_{2a}, \quad (9)$$

where θ_d is the diffracted angle of the reconstructed beam. From Eq. (7), it is apparent that either the refractive index or dimension shrinkage of the recording material leads to a shift in the Bragg angle $\Delta\theta_r$. The Bragg shift is dependent on the incident angles of the recording beams θ_{1a} and θ_{2a}. Here, we assume the parameters of the recording material as follows: $\alpha_l=0$, $\alpha_d=-1.5\%$, $\alpha_n=0.27\%$, and $d=20\,\mu$m. The Bragg angular shift $\Delta\theta_r$ as a function of the incident angles θ_{1a} and θ_{2a} is shown in Fig. 5. The maximum Bragg angular shift is about 0.8 deg in air when the incident angles are $\theta_{2a}=0$ and $\theta_{1a}=60$ deg. Our simulation results also show that when the recording geometry is symmetric (i.e., $\theta_{1a}=\theta_{2a}$), the Bragg angular shift is zero despite the shrinkage effect along the z axis. Thus, to avoid the Bragg angular shift produced by the thickness shrinkage, we can record the grating by using symmetric recording beams. In addition, the angular shift of the diffracted beam can be obtained by using Eq. (9). Thus, the CCD can be preshifted to the position such that the reconstructed data from holograms are detected correctly.

2.2 *Reflection Holograms*

2.2.1 *Angular shift of the reconstructed beam*

A schematic diagram of the geometry for the reflection holographic recording is shown in Fig. 6(a). In the figure, the angles are measured outside the medium. θ_{1a} and θ_{2a} are the angles between the reference beam and object beam with respect to the surface of the sample, respectively. Before optical recording, the original thickness and the transverse dimension of the recording material are d and l, respectively. λ is the wavelength for the recording and reading light, and n is the refractive index of the sample

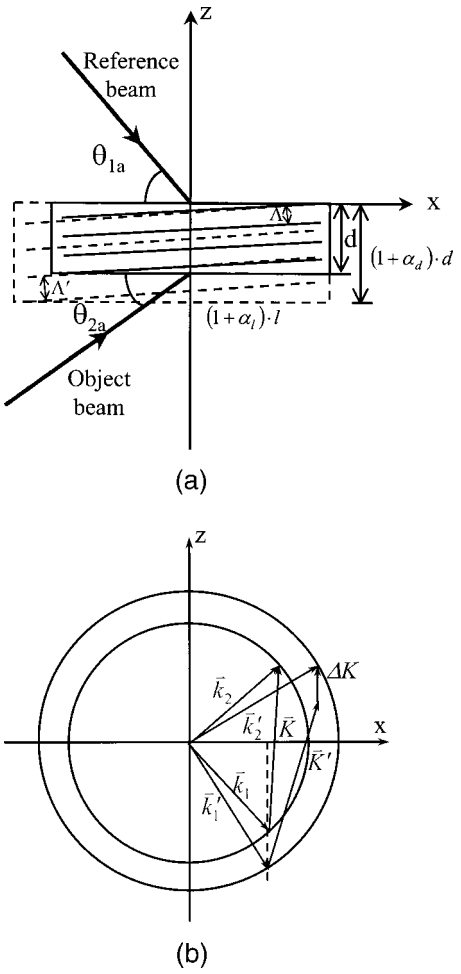

Fig. 6 Schematic diagram for recording reflection holograms, and (b) *K* diagram for the reflection hologram.

during recording. Two recording beams were incident onto the medium and the interference pattern is recorded. The grating wave vector can be written as[11]:

$$\vec{K}=\vec{k}_2-\vec{k}_1=\frac{2\pi}{\Lambda}(\sin\theta_0\hat{x}+\cos\theta_0\hat{z}), \tag{10}$$

where $\theta_0=(\theta_1-\theta_2)/2$. Λ is the grating spacing and is given by

$$\Lambda=\frac{\lambda}{2n\sin\left(\dfrac{\theta_1+\theta_2}{2}\right)}, \tag{11}$$

where θ_1 and θ_2 are the incident angles of the reference beam and object beam inside the medium, respectively. According to Snell's law, they can be written as $\theta_1=\cos^{-1}[\cos(\theta_{1a})/n]$ and $\theta_2=\cos^{-1}[\cos(\theta_{2a})/n]$.

We assume that after the holographic recording procedure is complete, because of the shrinkage effect, the material dimensions have changed to $(1+\alpha_d)\cdot d$ and $(1+\alpha_l)\cdot l$, and the refractive index of the material has changed to $(1+\alpha_n)\cdot n$. Then, the grating vector will be changed to

$$\vec{K}'=\frac{2\pi}{\Lambda}\left(\frac{1}{1+\alpha_l}\sin\theta_0\hat{x}+\frac{1}{1+\alpha_d}\cos\theta_0\hat{z}\right). \tag{12}$$

Thus, the Bragg matching condition will be changed. If the reading beam is incident at an angle identical to that of the recording beam, then the *k* diagram is shown in Fig. 6(b). There is a phase mismatch ΔK along the *z* axis, which can be written as:

$$\begin{aligned}\Delta K&=k'_{1z}+K'_z-k_{dz}\\&=\frac{2\pi}{\lambda}\left(-\{[(1+\alpha_n)n]^2-\cos^2\theta_{1a}\}^{1/2}-\frac{n}{1+\alpha_d}\right.\\&\quad\times[\sin\theta_1+\sin\theta_2]-\left\{[(1+\alpha_n)n]^2\right.\\&\quad\left.\left.-\left[\cos\theta_{1a}+\frac{1}{1+\alpha_l}(\cos\theta_{2a}-\cos\theta_{1a})\right]^2\right\}^{1/2}\right),\end{aligned} \tag{13}$$

where k'_{1z} is the wave vector of the reading beam along the *z* axis. k_{dz} is the wave vector of the reconstructed beam along the *z* axis and $k_{dz}=-\{[2\pi n(1+\alpha_n)/\lambda]^2-(k_{dx})^2\}^{1/2}$, where $k_{dx}=k'_{1x}+K'_x$. The angular shift of the diffracted beam is given by:

$$\begin{aligned}\Delta\theta_d&=\theta'_{2a}-\theta_{2a}\\&=\cos^{-1}\left[\cos\theta_{1a}+\frac{1}{1+\alpha_l}(\cos\theta_{2a}-\cos\theta_{1a})\right]-\theta_{2a},\end{aligned} \tag{14}$$

where θ'_{2a} is the diffracted direction after the shrinkage. Equation (14) indicates that the diffracted angle depends only on α_l and the recording angles. If $\alpha_l=0$, the shift of the diffracted angle is equal to zero. On the other hand, if there is shrinkage along the lateral dimension of the recording material, i.e., $\alpha_l\neq 0$, then the diffracted angles are affected. The computer simulation results for the case of $\alpha_l=-1\%$, $\alpha_d=-1\%$, $\alpha_n=-1\%$, and $d=100\,\mu$m, are shown in Fig. 7. The diffracted beam can deviate significantly (the angular shift can be as large as -7.15 deg) especially when the incident angle of the object beam is large ($\theta_{2a}\approx 0$ deg) and that of the reference beam is small ($\theta_{1a}\approx 80$ deg). In this case, if the positions of the CCD pixels are not adjusted to appropriate positions, then the diffracted pattern will not be detected correctly by the corresponding pixels. Therefore, we should either select appropriate incident angles of the recording beams to reduce the shrinkage effect, or shift the photodetector pixel to a suitable position to obtain a correct data detection.

2.2.2 *Degradation of the diffraction efficiency*

The diffraction efficiency for a Bragg-mismatched volume grating can be expressed as[11]

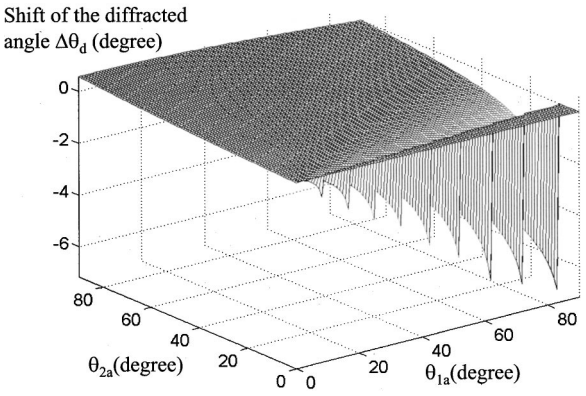

Fig. 7 Simulation results of the diffracted angle shift $\Delta\theta_d$ as a function of the incident angles θ_{1a} and θ_{2a}.

$$\eta = \frac{|\kappa|^2 \sinh^2(s\cdot t)}{s^2\cosh^2(s\cdot t) + \left(\frac{\Delta K}{2}\right)^2 \sinh^2(s\cdot t)}, \tag{15}$$

where $s=[|\kappa|^2-(\Delta K/2)^2]^{1/2}$ and $|\kappa|=\pi\Delta n/2\lambda \sin\theta_1$. It is seen that the diffraction efficiency will always be degraded even if $\alpha_l=0$, depending on the recording angles θ_{1a} and θ_{2a}. The simulation results are shown in Fig. 8. The parameters of the material that we used for this calculation are the following: $\alpha_l=0$, $\alpha_d=-1\%$, $\alpha_n=1\%$, and $d=100\,\mu$m. Figure 8 shows that the diffraction efficiency could be degraded significantly if the recording angles $(\theta_{1a},\theta_{2a})$ are less than 70 deg. Hence, to obtain high and uniform diffraction efficiency, we should choose large recording angles.

Let us perform a practical calculation. Assume that the center of the object beam is normally incident onto the recording material ($\theta_{2a}\approx 90$ deg), and the size of the input SLM is 13.2 mm. The pixel size of the input device is 33 μm and each row has 400 pixels. The focal length of the Fourier lens is 40 cm. This means that the range of the incident angles is from 89.13 to 90.87 deg. The focal length of the inverse Fourier lens is 20 cm. The pixel size of the CCD detector is 15 μm. The parameters of the DuPont HRF-800×071 photopolymer are the following: $n=1.5285$, $\alpha_n=0.27\%$, $d=20\,\mu$m, and $\alpha_d=-1.5\%$. The position shift and the diffraction efficiency of the reconstructed pixels are shown in Fig. 9. Both the two quantities depend on the incident angles of the reference beam. Figure 9(a) shows that the shift of output image is smaller with small reference angles ($\theta_{1a}=80$ deg). These simulation results have a tendency to be opposite the results of Fig. 7, because of the different parameters of the photopolymer materials. In principle, for a given photopolymer, we should use Eqs. (14) and (15) to find the suitable recording conditions of the holographic system to achieve the minimum detuning effect. Note that the diffraction efficiency of reflection holograms is very low at the Bragg mismatch. This problem can be alleviated by a precompensation method through adjusting the incident angle of the reading beam. The required angular shift of the reading beam for the Bragg matching condition is described in the following section.

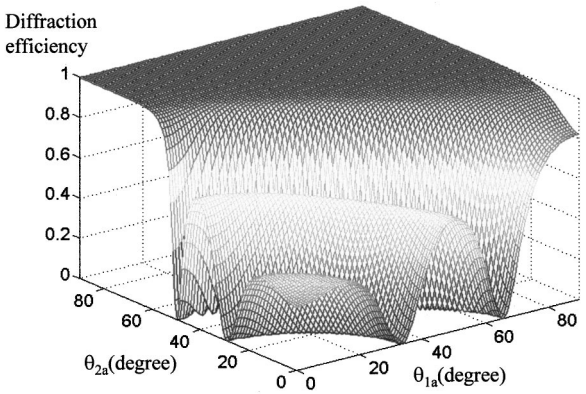

Fig. 8 Simulation results of the diffraction efficiency η as a function of the incident angles θ_{1a} and θ_{2a}.

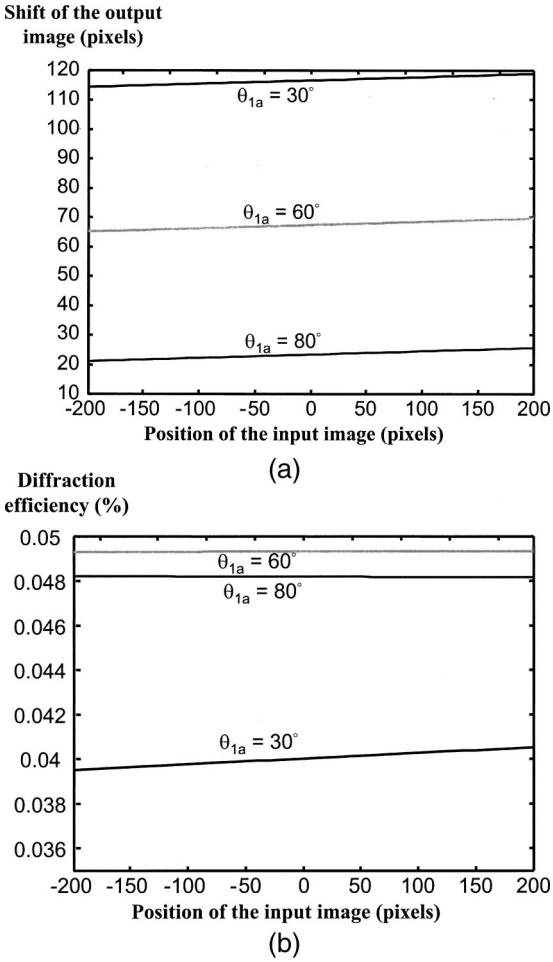

Fig. 9 (a) The position shift of the reconstructed image as a function of the image pixels with different incident angles $\theta_{1a}=80$, 60, and 30 deg. (b) The diffraction efficiency of the reconstructed image as a function of the image pixels with different incident angles $\theta_{1a}=80$, 60, and 30 deg.

2.2.3 *Precompensation by angular-shift of the reading beam*

Reconstruction of the volume grating at the Bragg matching condition can be achieved by a precompensation pro-

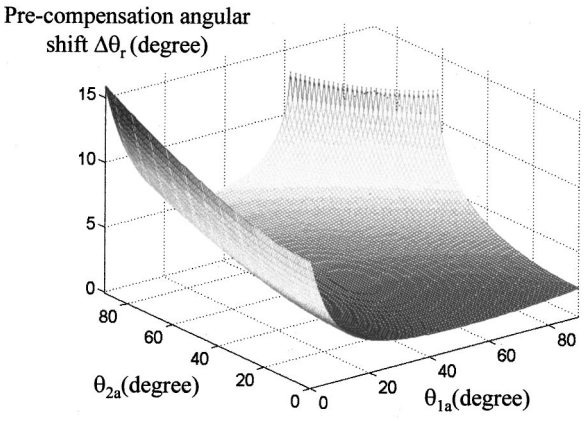

Fig. 10 Simulation results of the precompensation angular shift $\Delta\theta_r$ as a function of the incident angles θ_{1a} and θ_{2a}.

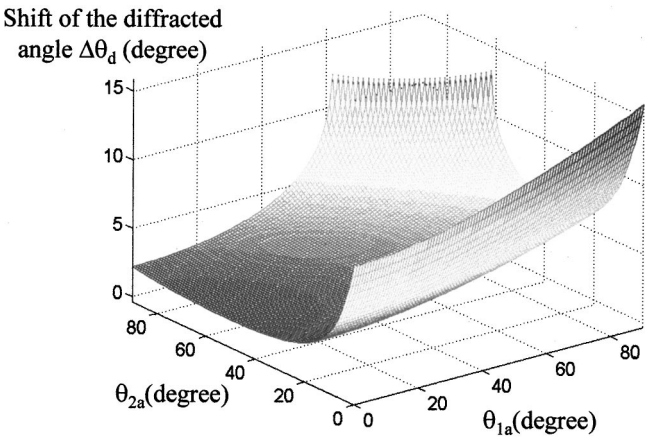

Fig. 11 Simulation results of the diffracted angle shift $\Delta\theta_r$ as a function of the incident angles θ_{1a} and θ_{2a}.

cess in which the incident angle of the reading beam is adjusted such that the phase mismatch ΔK is equal to zero. According to the condition of conservation of grating momentum, the angular shift of the precompensated reading beam can be derived as

$$\Delta\theta_r = \theta'_{1a} - \theta_{1a} = \cos^{-1}\left\{(1+\alpha_n)n\cdot\cos\left[\sin^{-1}\left(\frac{\lambda}{2(1+\alpha_n)n\Lambda'}\right) + \tan^{-1}\left(\frac{1+\alpha_d}{1+\alpha_l}\tan\theta_0\right)\right]\right\} - \theta_{1a}, \tag{16}$$

where θ'_{1a} is the reading angle for the Bragg matching condition, θ_{1a} is the recording angle, and Λ' is the grating spacing after optical recording. Λ' can be expressed as:

$$\Lambda' = \frac{\Lambda}{\left[\left(\frac{1}{1+\alpha_l}\sin\theta_0\right)^2 + \left(\frac{1}{1+\alpha_d}\cos\theta_0\right)^2\right]^{1/2}}. \tag{17}$$

Now the reading beam satisfies the Bragg condition, hence the maximum diffraction efficiency can be achieved. On the other hand, the diffracted angle will be deviated from the object beam direction, and the shift of the diffracted angle can be derived as

$$\Delta\theta_d = \theta_d - \theta_{2a} = \cos^{-1}\left\{(1+\alpha_n)n\cos\left[\sin^{-1}\left(\frac{\lambda}{2(1+\alpha_n)n\Lambda'}\right) - \tan^{-1}\left(\frac{1+\alpha_d}{1+\alpha_l}\tan\theta_0\right)\right]\right\} - \theta_{2a}, \tag{18}$$

where θ_d is the diffracted angle of the reconstructed beam. By using Eq. (16), the angular shift of the precompensated reading beam can be plotted as a function of the recording angles, as shown in Fig. 10. The parameters of the material that we used for calculation are the following: $\alpha_1 = 0$, $\alpha_d = -1.5\%$, $\alpha_n = 0.27\%$, and $d = 20\,\mu$m. Figure 10 shows that angular shift of the precompensated beam can be large (as large as 15.87 deg) with large reference angles (when $\theta_{1a} \leqslant 10$ deg). By using Eq. (18), the angular shift of the diffracted beam as a function of the recording angles can be obtained, as shown in Fig. 11. The angular shift of the diffracted beam depends on the incident angles of the object beam (θ_{2a}) and the reference angles (θ_{1a}). For holographic data storage by an angular multiplexing technique, the incident angle of the object beam for all data pages is fixed at one angle (θ_{2a}), while the incident angles of the reference beams (θ_{1a}) are different for each data page. In this situation, the angle shift for each reconstructed data page is different. Thus, the CCD can be preshifted to the position, such that the reconstructed data from all holograms are detected correctly. Thus, the detuning effect of a photopolymer volume holographic memory can be compensated by deviating the reading beam to the precompensating angle and at the same time by moving the CCD array to the appropriate diffracted place.

3 Optical Experiment

We first measured the parameters of the DuPont HRF-800 $\times 071$ photopolymer. The refractive indices (n and n') of the photopolymer before and after optical recording are measured with an Abbe refractometer. The measured results are $n = 1.5285$ and $n' = 1.5326$. Therefore, the fractional change in refractive index can be evaluated as $\alpha_n = (n' - n)/n = 0.27\%$. Next, by putting the photopolymer film in one arm of the Mach-Zehnder interferometer, the optical path difference of the photopolymer before and after optical exposure can be obtained. Since the original thickness of the photopolymer film is known to be 20 μm, the fractional change in the path difference and thus the fractional change of the thickness can be obtained as $\alpha_d = -1.5\%$.

The schematic diagram for recording and reading reflection-type holographic gratings is shown in Fig. 12. An argon laser beam is expanded and split into two plane waves. One (the reference beam) passes through a 4f system and the other one (the object beam) is incident directly onto the photopolymer film. The two beams interfere in the medium and the interference fringes are recorded in the photopolymer.

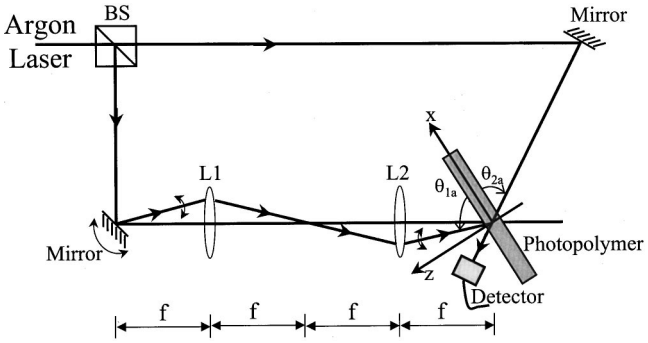

Fig. 12 A schematic diagram for reflection type holographic storage.

We have recorded reflection gratings with a symmetric incident geometry, i.e., $\theta_{1a}=\theta_{2a}$ (it means $\theta_0=0$ deg). According to Eq. (17), the grating spacing after optical recording only depends on the fraction of shrinkage of the material along the *z*-axis α_d. Equation (18) shows that this arrangement has the advantage of eliminating the infuence of the dimensional shrinkage of material along the *x* axis. After recording, the object beam is blocked and the reference beam is used as the reading beam. A photodetector is put at the position corresponding to the object beam direction for measuring the diffraction efficiency of the reconstructed beam. Because of the shrinkage effect, the Bragg condition is no longer satisfied and the diffraction efficiency is decreased. To find the Bragg angle, we adjusted the incident angle of the reading beam by using the 4f system until the highest diffraction efficiency is obtained. The deviation of the beam from the recording angle gives the angular shift. We measured the shift of the Bragg angle as a function of the incident angles of the recording beam. The results are shown in Fig. 13.

In Fig. 13, the solid line is the simulation result by using Eq. (18) and this curve is identical to the curve in Fig. 10 for the case $\theta_{1a}=\theta_{2a}$. The circled points are the experimental results. The experimental results match well with the computer simulation.

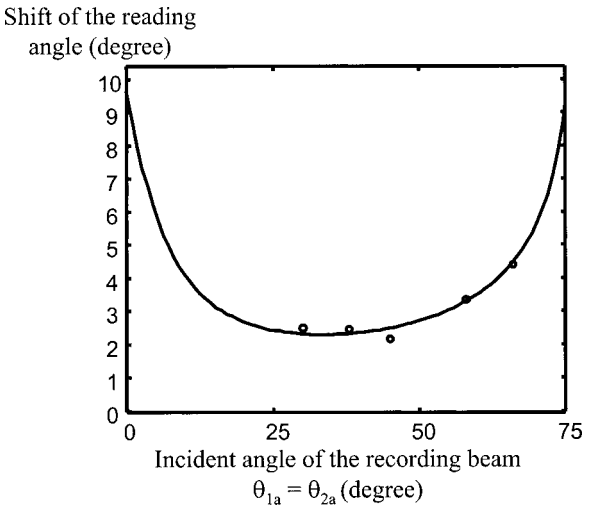

Fig. 13 A comparison of the numerical and the experimental results.

4 Conclusions

In summary, we have derived equations for the detuning effect on the Bragg angle and the diffraction efficiency of the reconstructed image for both transmission and reflection holograms. These equations can be used to estimate the grating detuning effect induced by the material shrinkage, i.e., the shrinkage effect of photopolymer during optical recording of holographic memories, and the temperature-induced detuning effect in photorefractive crystals during the thermal fixing procedure. In addition, it can also be used to find appropriate recording and reading conditions, such that the accuracy of holographic data storage is maintained. The grating detuning effect can be compensated by deviating the reading beam at a suitable angle, and the recorded data can be correctly retrieved by shifting the CCD array to the appropriate place. An optical experiment for measuring the detuning effect on reflection holograms has been performed and demonstrated.

Acknowledgments

The authors are grateful for scientific discussions with Prof. Poch Yeh. This research is supported in partial by a grant from the National Science Council of ROC under contract No. NSC-89-2215-E-009-024, and in partial from a research program supported by the Ministry of Education under Grant 89-E-FA06-1-4. Dr. Mei-Li Hsieh is a Postdoctoral Research Fellow supported by the Lee and MTI Center for Networking Research at National Chiao Tung University.

References

1. *Selected Papers on Holographic Storage*, G. T. Sincerbox, Ed., SPIE Milestone Series, Vol. MS 95, SPIE Press Bellingham, WA (1994).
2. H. Y. Li and D. Psaltis, "Three-dimensional holographic disks," *Appl. Opt.* **33**, 3764–3774 (1994).
3. D. Psaltis and F. Mok, "Holographic memories," *Sci. Am.* **273**(5), 70–76 (1995).
4. P. Hariharan, *Optical Holography*, 2nd ed., Cambridge University Press, Cambridge (1996).
5. A. Tork, P. Pilot, and T. V. Galstian, "New photopolymer materials for holographic data storage," in *2000 Optical Data Storage Conference*, 138–140, IEEE Press, 2000.
6. L. Dhar, M. G. Schnoes, T. L. Wysocki, H. Bair, M. Schilling, and C. Boyd, "Temperature-induced changes in photopolymer volume holograms," *Appl. Phys. Lett.* **73**(10), 1337–1339 (1998).
7. M. G. Schnoes, L. Dhar, M. L. Schilling, S. S. Patel, and P. Wiltzius, "Photopolymer-filled nanoporous glass as a dimensionally stable holographic recording medium," *Opt. Lett.* **24**(10), 658–660 (1999).
8. R. Vre, J. Heanue, K. Gurkan, and L. Hesselink, "Transfer functions based on Bragg detuning effects for image-bearing holograms recorded in photorefractive crystals," *J. Opt. Soc. Am. A* **13**(7), 1331–1344, (1996).
9. X. Yi and P. Yeh, "Effect of grating detuning in holographic storage," Vol. 4, *CLEO/Pacific Rim '99*, 1175–1176, IEEE Press (1999).
10. R. M. Shelby, D. A. Waldman, and R. T. Ingwall, "Distortions in pixel-matched holographic data storage due to lateral dimensional change of photopolymer storage media," *Opt. Lett.* **25**(10), 713–715 (2000).
11. P. Yeh, *Introduction to Photorefractive Nonlinear Optics*, Chap. 2, Wiley and Sons, New York (1993).

Mei-Li Hsieh received her BS in electrophysics in 1994 and her MS and PhD degrees in electro-optical engineering in 1996 and 2000, respectively, all from the National Chiao Tung University in Taiwan. From January 1998 until December 1998, she was a guest researcher in the Visual Image Processing Group of Information Access and User Interfaces Division at the National Institute of Standards and Technology in Gaithersburg, Maryland. She is currently a post-doctoral research fellow in the Institute of Electro-Optical Engineering at the National Chiao Tung University. Her research areas are in holographic storage, optical computing, optical spatial light modulator devices, and optical image processing.

Ken Y. Hsu received his BS in electrophysics in 1973 and his MS in electronic engineering in 1975, both from the National Chiao Tung University in Taiwan. He received his PhD in electrical engineering from the California Institute of Technology in 1989. He is currently a professor in the Institute of Electro-Optical Engineering at the National Chiao Tung University. His research interests are in the areas of optical computing, optical neural networks, optical devices, and holography for information processing.